

Spectroscopy of Local Density of States Fluctuations in a Disordered Conductor

T. Schmidt, R. J. Haug*, Vladimir I. Fal'ko[†], and K. v. Klitzing

Max-Planck-Institut für Festkörperforschung, Heisenbergstr. 1, 70569 Stuttgart, Germany

A. Förster and H. Lüth

Institut für Schicht- und Ionentechnik, Forschungszentrum Jülich GmbH, Postfach 1913,

52428 Jülich, Germany

(September 8, 1995)

Abstract

The local density of states of a degenerate semiconductor is investigated at low magnetic fields by resonant tunneling through a discrete localized electron level. Fine structure in the tunneling current provides a temperature insensitive image of mesoscopic fluctuations of the local density of states below the Fermi level. The fluctuations are demonstrated to originate from quantum interference of diffusive electron waves in the three-dimensional disordered system.

Quantum mechanics is well known to manifest itself in the low-temperature transport properties of disordered conductors. Weak localization corrections to the conductivity [1] and universal conductance fluctuations [2] are the phenomena most explored experimentally in disordered metals. Their theoretical understanding is based on the interference of diffusive electron waves [1,3] which on one hand, suppresses quantum diffusion and, on the other hand, makes the transport properties sample-specific since the interference pattern depends on the configuration of disorder. Universal conductance fluctuations are entirely determined by the properties of electron states at the Fermi level. According to existing theory, however, fluctuations in the spectrum of levels as well as the structure of wavefunctions are reflected in full detail only in the density of states [4] and, especially, the local density of states (LDOS) [5] of disordered systems. Recently, the first LDOS observation was realized by employing scanning-tunneling microscopy to image the influence of an external modulation on the two-dimensional surface bands of noble metals [6]. In contrast, the experimental study of LDOS fluctuations in disordered three-dimensional conductors was impossible until now due to the lack of an appropriate spectrometer.

In this letter, we analyze the LDOS of a three-dimensional (3D) degenerate semiconductor by means of resonant tunneling through a discrete localized electron state. Resonant tunneling is known as a spectroscopic tool for probing the properties of electronic systems [7]. Recently, it has been proposed to employ resonant tunneling through impurity states for studying the LDOS in the contacts of metal-insulator-metal junctions [8]. The idea of our experiment is slightly different as illustrated by the sketch in Fig. 1. Electrons tunnel from the heavily-doped disordered emitter of a double-barrier heterostructure through the energetically-lowest level S in the quantum well which serves as *spectrometer* because it is narrow in energy and localized in space. Such discrete localized states were recently shown to have a defect-related origin [9]. The tunneling current I is determined by the transparency of the thick emitter barrier as well as by the *local tunneling density of states* ν in the emitter at the position of the spectrometer, $I \propto \nu$. As a bias voltage V is applied, the spectrometer scans the LDOS below the Fermi level as a function of energy.

The measured tunneling current exhibits an irregular modulation which reflects exclusively LDOS fluctuations, $\delta I \propto \delta \nu$, since the emitter-barrier transparency is a smooth function of energy. The observed fluctuation pattern is analyzed in detail as a function of bias voltage and magnetic field.

The experiment was performed using a strongly asymmetric double-barrier heterostructure grown by molecular-beam epitaxy on n^+ -type GaAs substrate. The structure consists of a 10 nm wide GaAs quantum well sandwiched between two $\text{Al}_{0.3}\text{Ga}_{0.7}\text{As}$ barriers of 5 and 8 nm width (top and bottom barrier). The undoped active region is separated from 300 nm thick GaAs contact layers doped with Si to $4 \times 10^{17} \text{ cm}^{-3}$ by 7 nm wide GaAs spacer layers. From this material we fabricated a pillar with a diameter of 500 nm supplied with ohmic top and bottom contacts. The current and the differential conductance of the device were independently measured in a dilution refrigerator. A lock-in amplification technique was used with an ac excitation voltage of 15 μV amplitude and 13 Hz frequency superimposed on the dc bias voltage applied to the top contact.

Figure 1 (a) shows the low-bias part of the current-voltage characteristic $I(V)$ measured at the base temperature of $T \approx 30 \text{ mK}$ of the dilution refrigerator. Two steps due to resonant tunneling through discrete levels are clearly observed. The first step in the current occurs at the voltage at which the energetically-lowest discrete state S in the quantum well crosses the electrochemical potential μ_E in the emitter contact, see sketch on top of Fig. 1. The voltage scale is related to the energy scale by $E = \alpha eV + \text{const}$ with $\alpha \approx 0.5$ denoting the voltage-to-energy conversion coefficient. The second step arises when the next, energetically higher discrete state becomes available for transport.

The most striking feature of the data is the reproducible oscillatory fine structure which is superimposed on the current plateau between the two current steps. Indications of similar fluctuations were recently observed by several groups [10–13]. The current plateau is formed by electrons which tunnel from below the emitter Fermi level through the lowest discrete state in the quantum well. The tunneling current depends on the transparencies of the barriers and the density of states in both contacts. In order to eliminate the influence of the

collector-barrier tunneling process, we designed the double-barrier heterostructure strongly asymmetric. The transparency of the thick emitter barrier is by orders of magnitude lower than that of the collector barrier. Hence, it is the emitter-tunneling process which determines the magnitude of the current. The observed fine structure represents thus a direct image of fluctuations of the density of states in the emitter contact, $\delta I \propto \delta \nu$. This image is recorded by using the energetically-lowest discrete state in the quantum well as spectrometer. The finite slope of the current plateau is due to the smooth bias-voltage dependence of the transparency of the emitter barrier [14].

The fine structure is even more pronounced in the simultaneously measured differential conductance $G = dI/dV$ plotted in Fig. 1 (b) for $T \approx 30$ mK and $T = 1.0$ K. Considering differential conductance instead of current eliminates the finite slope of the current plateaus. Large resonances in the differential conductance originate from the current steps in the $I(V)$ characteristic. The amplitude of these main resonances is sensitive to thermal broadening of the Fermi distribution since they are due to electrons tunneling from the Fermi level. In contrast, the fine structure is practically temperature independent. This independence complies with the assumption of resonant tunneling from below the Fermi level where at $T = 1.0$ K all emitter states are still occupied.

In order to investigate the quantum origin of the density of states fluctuations, we employed a magnetic field to vary the interference conditions for diffusive electron waves in the emitter contact. Figure 2 shows the differential conductance G as a function of both the bias voltage V and a magnetic field B parallel to the current flow. The position of the main resonances in bias is up to $B = 2$ T independent of the magnetic field, which demonstrates that the corresponding discrete electron states in the quantum well are strongly localized in space. Measurements up to higher fields yield a radius of $r \sim 10$ nm for the energetically-lowest state (in analogy to Ref. [14]) which suggests that the spectrometer is a single impurity within the double-barrier region. The spectral resolution of our experiment is deduced from the width of the first conductance resonance as $\gamma \approx 0.2$ meV. Since the *spectrometer* is strongly localized, it is the *local density of states* at the lateral position

of this discrete level which determines the oscillatory fine structure between the two main resonances. It is however important to realize that the differential conductance displays in contrast to the current not directly density of states fluctuations but their derivative with respect to energy, $\delta G \propto \delta(d\nu/dE)$. The fine structure shows a strong irregular dependence on magnetic field which is the subject of the following statistical analysis.

The analysis of the fluctuation pattern is based on the evaluation of correlation functions in the intervals $V = 25 - 30$ mV and $B = 0 - 2$ T. Fig. 3 (a) represents the autocorrelation function $\langle K_{\Delta B} \rangle_V = \langle \langle \delta G(B) \delta G(B + \Delta B) \rangle_B / \text{var}_B G \rangle_V$ as a function of magnetic field with $\delta G(B) = G(B) - \langle G(B) \rangle_B$ and $\text{var}_B G = \langle \delta G^2(B) \rangle_B$. The symbols $\langle \dots \rangle_V$ and $\langle \dots \rangle_B$ indicate averaging over bias voltage and magnetic field, respectively. The half width at half maximum gives us the correlation field B_c which is the quasi period of the fluctuations. The inset in Fig. 3 (a) shows that the correlation field $B_c \approx 0.1$ T is rather independent of the magnetic-field orientation θ with respect to the direction of the current. This independence proves the 3D origin of the fluctuation pattern and, thus, demonstrates the 3D character of the quantum states in the emitter contact. The Fourier transform of $\langle K_{\Delta B} \rangle_V$ is the power spectrum $\langle S_B \rangle_V$ of the fluctuations plotted in Fig. 3 (b). It decays exponentially over more than two orders of magnitude. A fit according to $\langle S_B \rangle_V \propto \exp(-f_B B_c)$ yields again $B_c \approx 0.1$ T. The autocorrelation function as a function of bias voltage $\langle K_{\Delta V} \rangle_B$ and the corresponding power spectrum $\langle S_V \rangle_B$ are plotted in Figs. 3 (c) and (d). The correlation voltage is $V_c \approx 0.3$ mV as taken from the autocorrelation function and $V_c \approx 0.5$ mV as obtained from an exponential fit to the power spectrum. This corresponds to a correlation energy of $E_c = \alpha e V_c \approx 0.2$ meV.

Figure 4 (a) shows the correlation field B_c as a function of bias voltage extracted from $K_{\Delta B}$ which was computed using individual magnetic-field traces of the differential conductance. The corresponding dependence of the correlation voltage V_c on magnetic field extracted from $K_{\Delta V}$ is plotted in Fig. 4 (b). The correlation field varies irregularly on the scale of V_c while the correlation voltage changes on the scale of B_c , which confirms the random character of the fine structure. The mean square of the fluctuations exhibits a similar behavior: Figures 4 (c) and (d) show that $\text{var}_B G$ changes on the scale of V_c , while $\text{var}_V G$

varies on the scale of B_c .

As the magnitude of the LDOS fluctuations is given by the magnitude of the current fluctuations, we plot in Figs. 5 (a) and (b) the normalized variance of the current as a function of bias voltage and magnetic field. The quantities $\text{var}_B I/I^2$ and $\text{var}_V I/I^2$ vary on a larger scale than $\text{var}_B G$ and $\text{var}_V G$ since they contain contributions of long-range fluctuations which are suppressed in the differential conductance. The autocorrelation functions and power spectra of the current data yield $B_c \approx 0.2$ T and $E_c \approx 0.4$ meV. From Fig. 5, the normalized variance of the LDOS fluctuations is determined to $\text{var}\nu/\nu^2 \propto \text{var}I/I^2 \approx 0.5 \times 10^{-2}$.

We discuss these results using the semiclassical picture of quantum interference between scattered electron waves. At zero magnetic field, the local fluctuation pattern of the density of states can be imagined as a superposition of the tails of Friedel oscillations extended from the closest impurities [15]. The magnetic field dependence of the LDOS fluctuations is formed by closed paths able to encircle magnetic flux as shown by the sketch in Fig. 5 [16]. The above determined correlation magnetic field agrees roughly with the value of $B_c \sim \phi_0/l^2 \approx 0.4$ T calculated with ϕ_0 the magnetic flux quantum and $l \approx 100$ nm the mean free path deduced from the doping density of the disordered contact. Thus, we conclude that the observed fluctuations are formed by semiclassical trajectories on the length scale of the mean free path, similar to weak localization corrections to the conductivity in 3D systems. It is however important to note that the LDOS exhibits no weak localization correction, i.e. the tunneling current and the magnitude of the main conductance resonances do not increase with growing magnetic field, see Fig. 2. The correlation energy of LDOS fluctuations generated on the length scale of the mean free path is theoretically expected to be $E_c \sim \hbar/\tau = \hbar(v/l)$ with τ the momentum relaxation time and v the Fermi velocity. From the sample parameters we estimate $E_c \sim 1$ meV which is of the same order of magnitude as experimentally observed. The theoretical expectation [5] for the amplitude of the LDOS fluctuations in 3D systems is $\text{var}\nu/\nu^2 \sim (\lambda/l)^2$ with λ being the Fermi wavelength. In our case a value of $(\lambda/l)^2 \sim 10^{-2}$ results in reasonable agreement with experiment. Finally, we want to point out that $\text{var}_V G$ exhibits a maximum at $B = 0$ T (Fig. 4 (d)) which is expected

for the magnitude of LDOS fluctuations due to breaking of the time-reversal symmetry in magnetic field.

In summary, we studied resonant tunneling through a discrete localized level in a semiconductor double-barrier heterostructure at low magnetic fields. Mesoscopic fluctuations of the local density of states in the emitter contact are observed as temperature insensitive fine structure in the tunneling current. The analysis of correlation functions and magnitude of the fine structure demonstrates, that the fluctuation pattern is generated by quantum interference of scattered electronic orbits at the length scale of the mean free path of the disordered bulk semiconductor.

We thank M. Tewordt and B. Schönherr for expert help during the sample fabrication and A. K. Geim and I. V. Lerner for helpful discussions. This work has been supported by the Bundesministerium für Bildung, Wissenschaft, Forschung und Technologie.

REFERENCES

- * New address: Institut für Festkörperphysik, Universität Hannover, Appelstr. 2, 30167 Hannover, Germany.
- † New address: Department of Theoretical Physics, Oxford University, OX1 3NP Oxford, UK.
- [1] G. Bergmann, Phys. Rep. **107**, 1 (1984); P. A. Lee and T. V. Ramakrishnan, Rev. Mod. Phys. **57**, 287 (1985).
- [2] S. Washburn and R. A. Webb, Adv. Phys. **35**, 375 (1986).
- [3] For a review see *Mesoscopic Phenomena in Solids*, edited by B. L. Altshuler, P. A. Lee and R. A. Webb (North-Holland, Amsterdam, 1991).
- [4] B. L. Altshuler and B. I. Shklovskii, Zh. Eksp. Teor. Fiz. **91**, 220 (1986) [Sov. Phys. JETP **64**, 127 (1986)].
- [5] I. V. Lerner, Phys. Lett. A **133**, 253 (1988); B. L. Altshuler, V. E. Kravtsov and I. V. Lerner, p. 449 in Ref. [3].
- [6] M. F. Crommie, C. P. Lutz and D. M. Eigler, Nature **363**, 524 (1993); Science **262**, 218 (1993); E. J. Heller, M. F. Crommie, C. P. Lutz and D. M. Eigler, Nature **369**, 464 (1994).
- [7] U. Sivan, F. P. Milliken, K. Milkove, S. Rishton, Y. Lee, J. M. Hong, V. Boegli, D. Kern and M. DeFranza, Europhys. Lett. **25**, 605 (1994).
- [8] I. V. Lerner and M. E. Raikh, Phys. Rev. B **45**, 14036 (1992).
- [9] M. W. Dellow, P. H. Beton, C. J. G. M. Langerak, T. J. Foster, P. C. Main, L. Eaves, M. Henini, S. P. Beaumont and C. D. W. Wilkinson, Phys. Rev. Lett. **68**, 1754 (1992); M. Tewordt, L. Martín-Moreno, V. J. Law, M. J. Kelly, R. Newbury, M. Pepper, D. A. Ritchie, J. E. F. Frost and G. A. C. Jones, Phys. Rev. B **46**, 3951 (1992).

- [10] B. Su, V. J. Goldman and J. E. Cunningham, *Science* **255**, 313 (1992); *Phys. Rev. B* **46**, 7644 (1992).
- [11] A. K. Geim, P. C. Main, N. La Scala, Jr., L. Eaves, T. J. Foster, P. H. Beton, J. W. Sakai, F. W. Sheard, and M. Henini, *Phys. Rev. Lett.* **72**, 2061 (1994).
- [12] M. R. Deshpande, E. S. Hornbeck, P. Kozodoy, N. H. Dekker, J. W. Sleight, M. A. Reed, C. L. Fernando and W. R. Frensley, *Semicond. Sci. Technol.* **9**, 1919 (1994).
- [13] P. J. McDonnell, A. K. Geim, P. C. Main, T. J. Foster, P. H. Beton and L. Eaves, *Physica B* **211**, 433 (1995).
- [14] T. Schmidt, M. Tewordt, R. J. Haug, K. v. Klitzing, A. Förster and H. Lüth, *Solid State Electron.*, in press.
- [15] D. Pines and P. Nozières, *The Theory of Quantum Liquids* (Plenum, New York, 1966).
- [16] In our limit of low magnetic fields, the cyclotron frequency is smaller than the momentum relaxation rate of the electrons in the doped contact, $\omega_c\tau \leq 1$. Hence, Landau quantization has not to be considered and the semiclassical picture of scattered electron waves is applicable. In the opposite limit of high magnetic fields, $\omega_c\tau \gg 1$, the irregular fluctuation pattern analyzed in this paper becomes more regular, as has been observed recently by different groups (see M. R. Deshpande *et al.*, p. 1899 in *22nd International Conference on the Physics of Semiconductors*, edited by D. J. Lockwood (World Scientific, Singapore, 1995), as well as Refs. [11] and [14]).

FIGURES

FIG. 1. (a) Current-voltage characteristics $I(V)$ measured at $T \approx 30$ mK (a). (b) Oscillations of the differential conductance $G = dI/dV$ recorded at $T \approx 30$ mK (solid) as well as $T = 1.0$ K (dotted). The schematical drawing on top illustrates the spectroscopy of the local density of states in the disordered emitter contact of a double-barrier heterostructure.

FIG. 2. Differential conductance vs bias voltage and magnetic field (step 0.01 T) as surface plot (a) and color map (b) (white, $G \leq -0.08 \mu\text{S}$; black, $G \geq 0.10 \mu\text{S}$).

FIG. 3. Voltage-averaged autocorrelation function (a) and power spectral density (b) in magnetic field; field-averaged autocorrelation function (c) and power spectral density (d) in voltage ($V = 25 - 30$ mV and $B = 0 - 2$ T). The inset of (a) shows the correlation field as function of the magnetic-field orientation θ with respect to the direction of the current. The solid lines in (b) and (d) are exponential fits to the power spectra.

FIG. 4. Correlation field vs bias voltage (a) and correlation voltage vs magnetic field (b); variance of the differential conductance $\text{var}_B G = \langle \delta G^2(B) \rangle_B$ vs bias voltage (c) and $\text{var}_V G = \langle \delta G^2(V) \rangle_V$ vs magnetic field (d).

FIG. 5. Normalized variance of the current $\text{var}_B I/I^2$ vs bias voltage (a) and $\text{var}_V I/I^2$ vs magnetic field (b). Average values are given by dashed lines. The sketch on top visualizes a typical closed electron trajectory responsible for fluctuations of the local density of states.

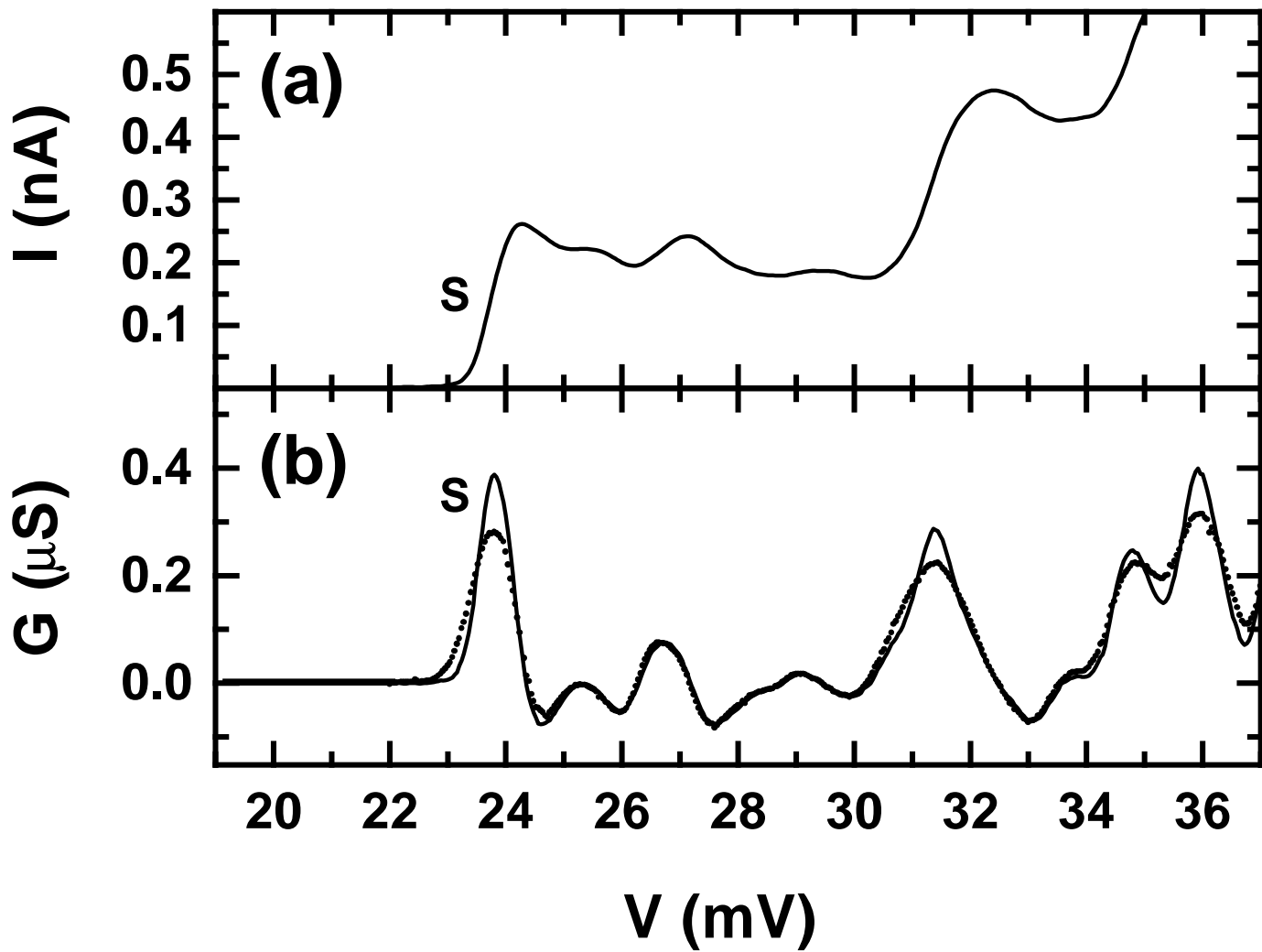
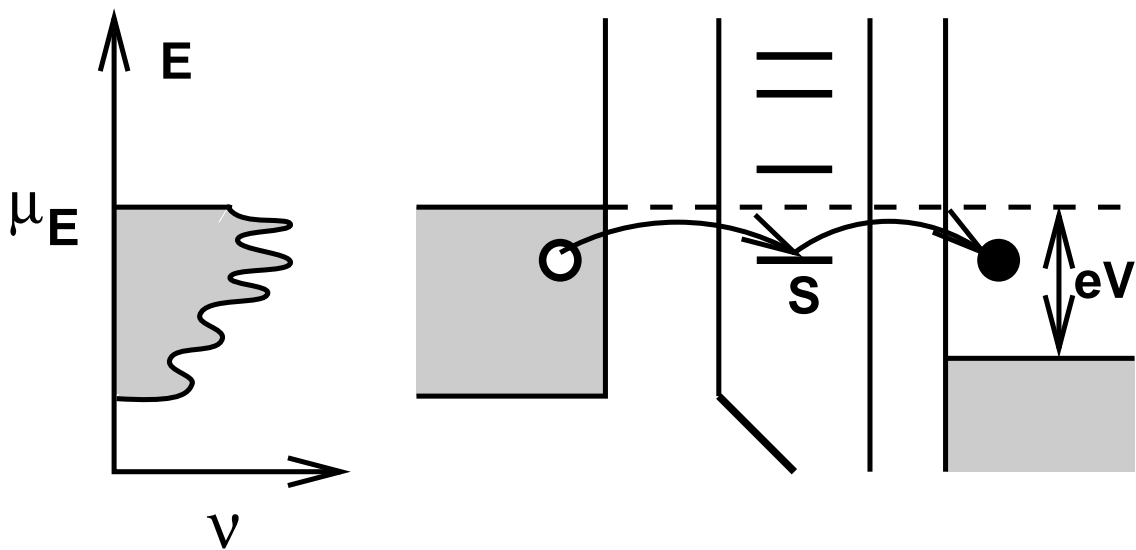


Fig. 1, Schmidt et al.

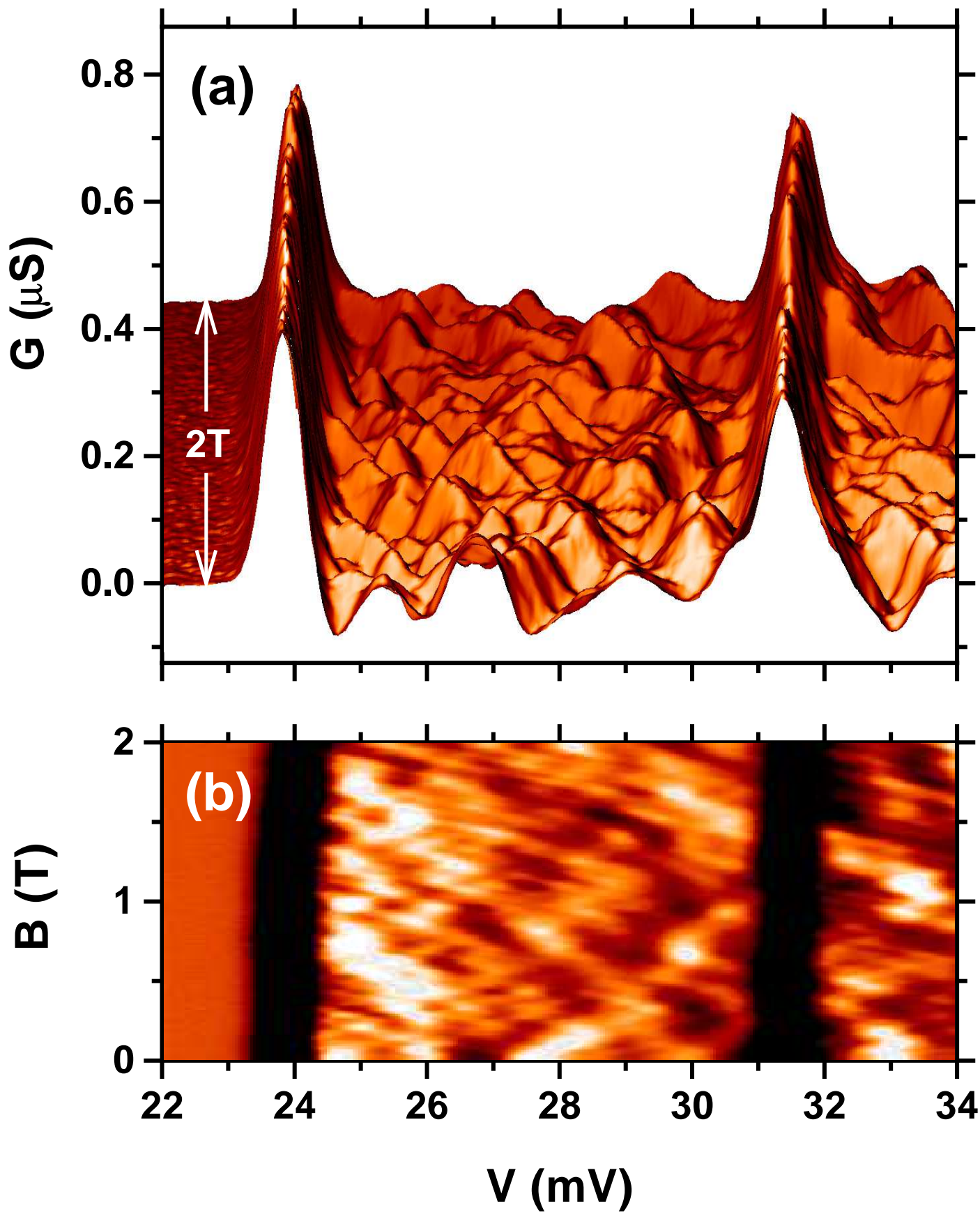


Fig. 2, Schmidt et al.

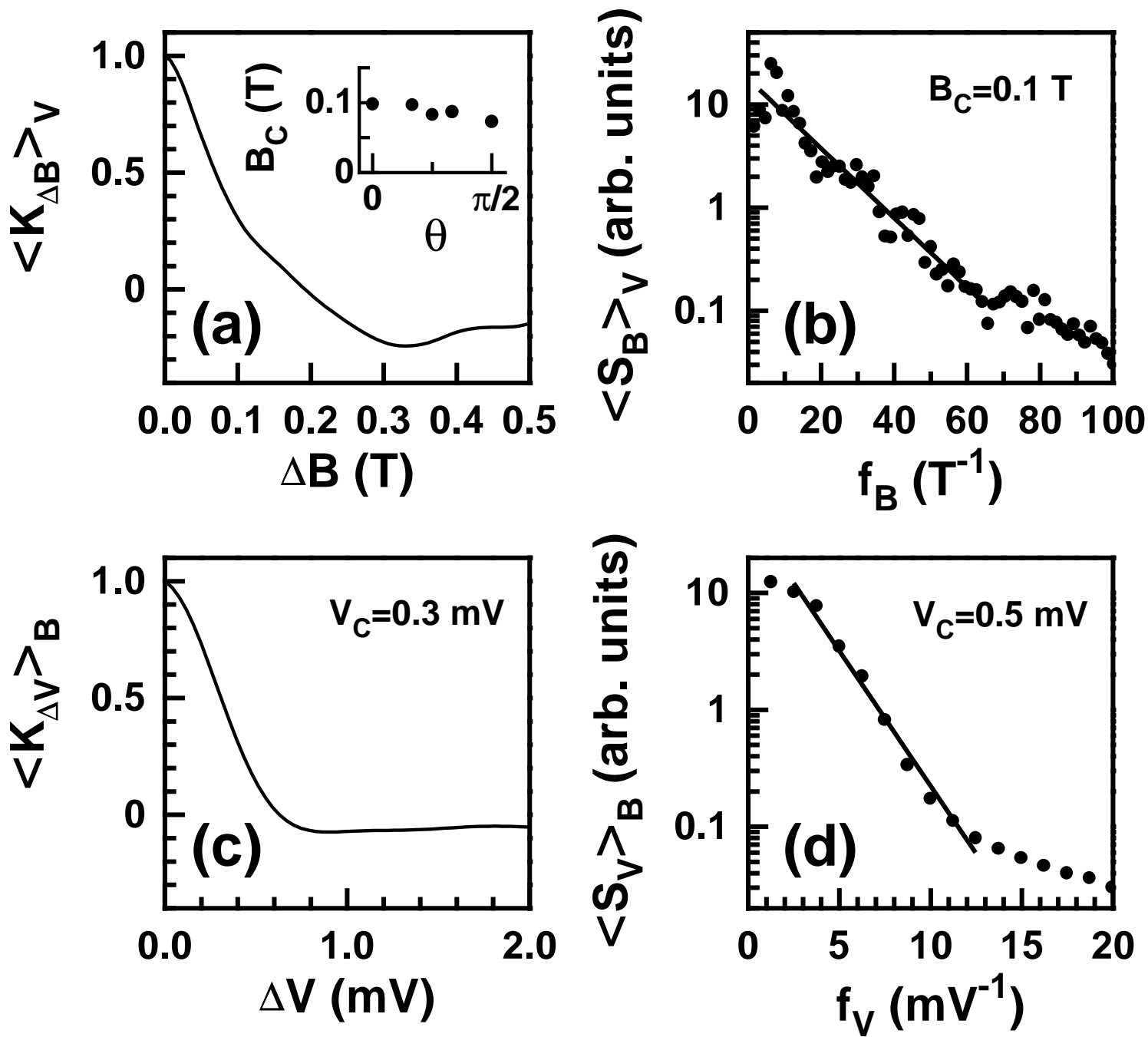


Fig. 3, Schmidt et al.

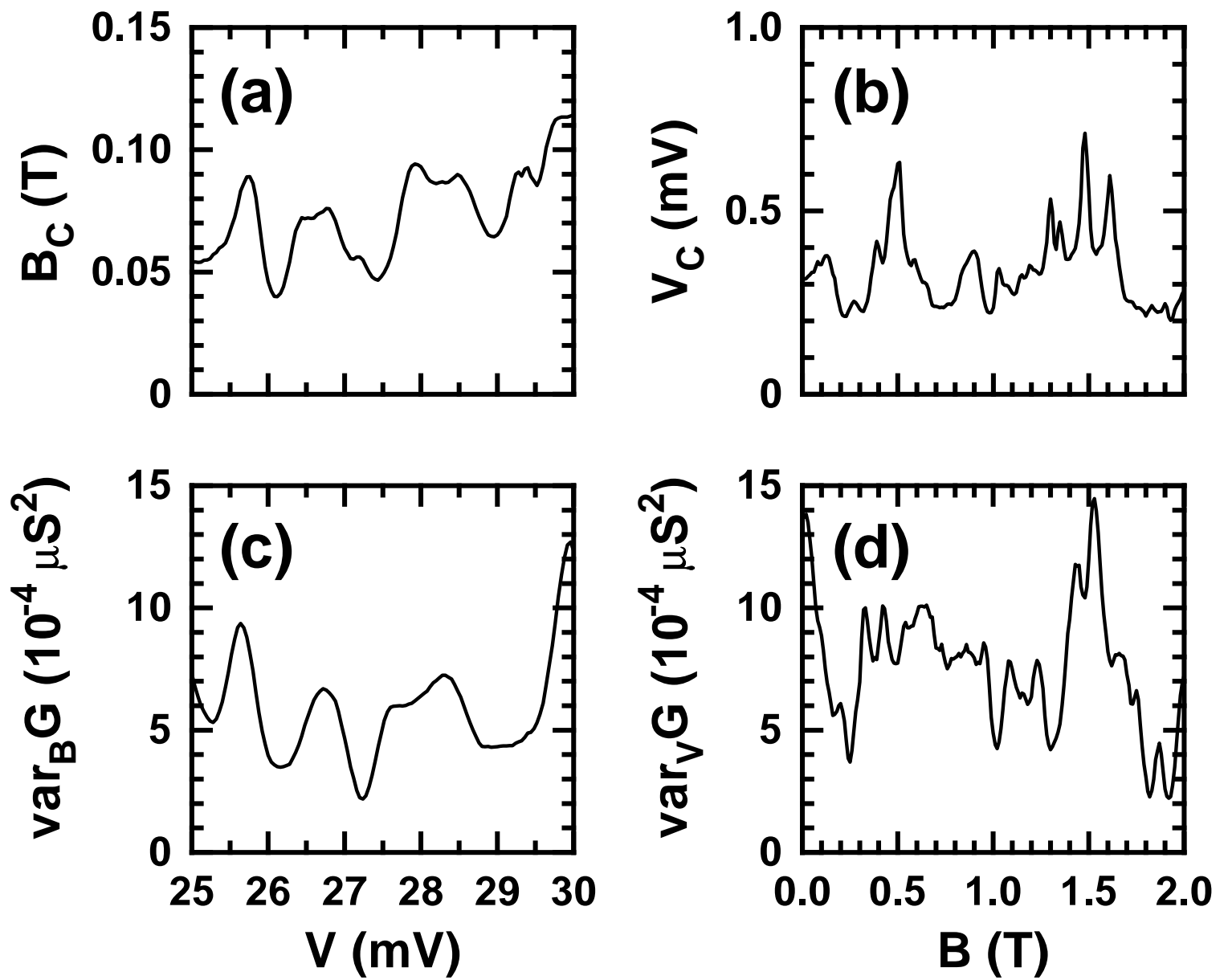


Fig. 4, Schmidt et al.

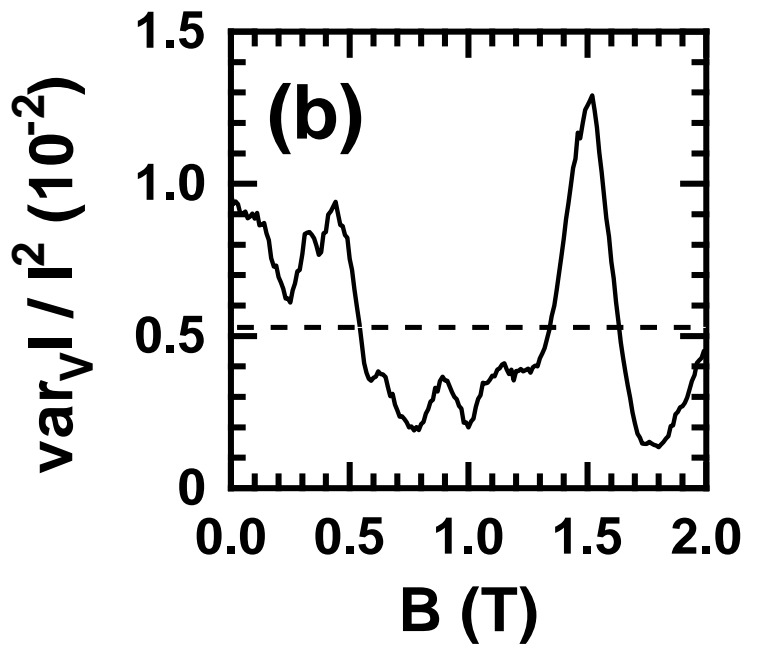
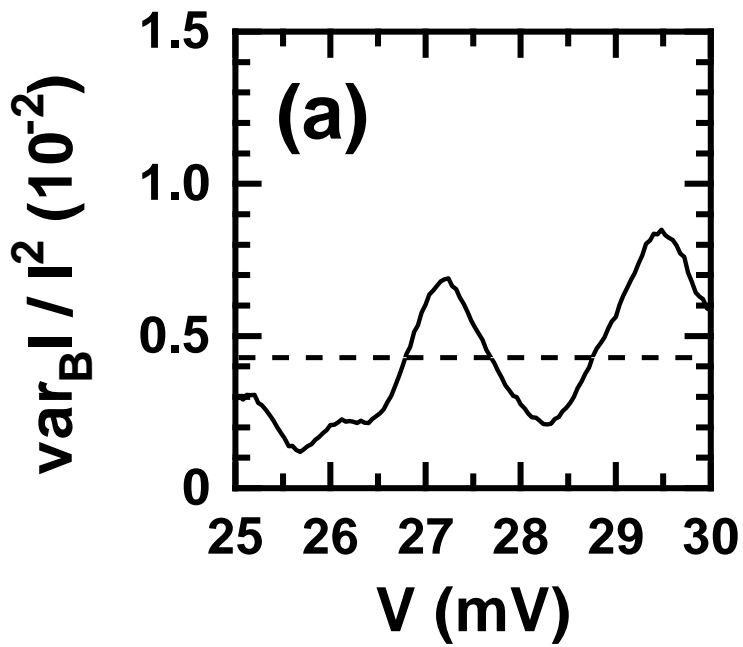
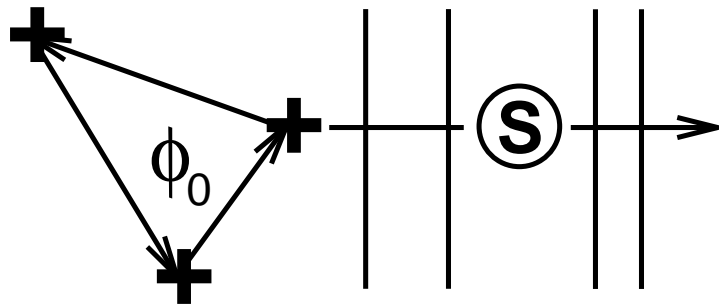


Fig. 5, Schmidt et al.